

# Physical model of CdS-based thin-film photovoltaic junctions

M. L. C. Cooray<sup>a)</sup> and V. G. Karpov

Department of Physics and Astronomy, University of Toledo, Toledo, Ohio 43606

(Received 18 November 2005; accepted 17 January 2006; published online 28 February 2006)

We propose a simple physical model of CdS-based thin-film photovoltaic junctions including the major types that utilize the CdTe and Cu(In,Ga)Se<sub>2</sub> absorber layers. This model allows for field reversal in the CdS layer. It is solved analytically, verified numerically, and predicts a variety of phenomena, such as the lack of carrier collection from CdS, buffer layer effects, light to dark current-voltage curve crossing and rollover. © 2006 American Institute of Physics. [DOI: 10.1063/1.2181201]

The technology of polycrystalline thin-film photovoltaics (PV) has reached a degree of maturity allowing its industrial scaleup and market development.<sup>1,2</sup> However, understanding of these device operations remains insufficient and lacking explanations of many important facts. For example, two major types of thin-film PV based on CdTe and Cu(In,Ga)Se<sub>2</sub> (CIGS) absorbers, use a thin layer of CdS, whose role remains puzzling. In particular, it causes a substantial blue light absorption ( $\hbar\omega > 2.4$  eV) without any contribution to the carrier collection, which contradiction, while commonly recognized, does not have a good explanation. Several other controversial observations are listed below. This lack of physical understanding leaves the technology with rather inefficient trial-and-error approaches.

Here, we present a physical model that at least semi-quantitatively explains all the significant facts related to CdS-based thin-film PV, allows for a closed analytical solution (verified numerically), and predicts different possibilities in device manufacturing.

As a brief introduction, we note that the prevailing model of CdS-based PV have been a *p-n* junction with CdS layer as the *n*-type component. The model parameters include layer thicknesses, band offsets (between CdS, CdTe, and contact metals), doping concentrations, and some others specified by the existing software packages, such as AMPS.<sup>3,4</sup> The current-voltage (*J-V*) curve fitting is considered a major test for this type of modeling.

However, *J-V* modeling as such appears not conclusive enough, since reasonable fits can be obtained with different models (Fig. 1). This is not surprising: the diode-type *J-V*s naturally occur with any barrier dominated electron transport. As a result different structures with multiple fitting parameters (and often with more than one barrier) can provide comparable fits. Other indicative observations are needed to verify the device model.

A list of such indicative observations below limits model choice to that of Fig. 2. (1) The pressure dependent PV performance attributable to the piezoparameters of CdS (Ref. 5) suggests a strong electric field in the depleted CdS layer. The energetically favorable CdS electric dipole orientation requires that this field be opposing the average device field. (2) The “reach-through” band bending in CdTe caused by a buffer layer on the other side of CdS (Refs. 6 and 7) suggests the metal-insulator-semiconductor nature of the device with

an insulating CdS. (3) Pointing at the same is that using more conductive CdS does not improve the device. To the contrary, a rather insulating chemical bath deposited CdS is used in high-quality PV.<sup>2</sup> (4) Buffer layers of certain morphology (for example, sputtered) strongly increase the device open-circuit voltage ( $V_{oc}$ ), while other chemically and electrically equivalent layers (such as chemical vapor deposited) do not cause this effect.<sup>6,7</sup> This points to the role of interfacial morphology and possibly its related internal stress acting through the piezoeffect.<sup>5</sup> (5) Absence of carrier collection from CdS (Ref. 2) may suggest the electric-field reversal in CdS relative to that in CdTe or CIGS layers [consistent with the above item (1)]. (6) Pointing to the same is the negative quantum efficiency,  $QE < 0$  observed under the blue illumination and zero bias for devices with thick CdS.<sup>8</sup> (7) Light and dark *J-V* crossover pointing at CdS related photoconductivity,<sup>9</sup> and light *J-V* rollover in the fourth quadrant.<sup>2</sup>

The diagram in Fig. 2 is consistent with all of the above observations. Its unique feature is the electric-field reversal and “gull wing” singularity in the conduction band implying positive interfacial charges (due to the piezoeffect or defect states, or both). Following Ref. 3, we do not assume any significant band offset between the CdS and its tangent layers; however, adding a moderate offset does not change the model predictions. Also, we do not specify the band bending

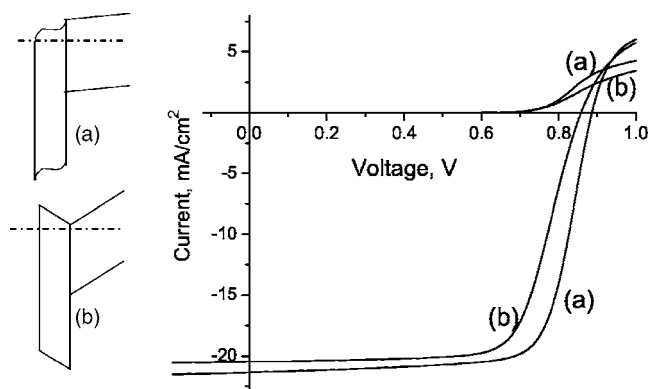


FIG. 1. AMPS generated light and dark *J-V* characteristics for two different device models: The standard *p-n* junction (a), and this work model (b). For the case (a), we used the device parameters (suggested in Ref. 3) including the back barrier, but without the buffer layer and deep defects in CdS. For the case (b), the reversed electric field was additionally introduced by creating two heavily doped ( $10^{18}$  cm<sup>-3</sup>) interfacial layers and decreasing the carrier concentration in CdS to  $2 \times 10^{16}$  cm<sup>-3</sup>.

<sup>a)</sup>Electronic mail: lcooray@physics.utoledo.edu

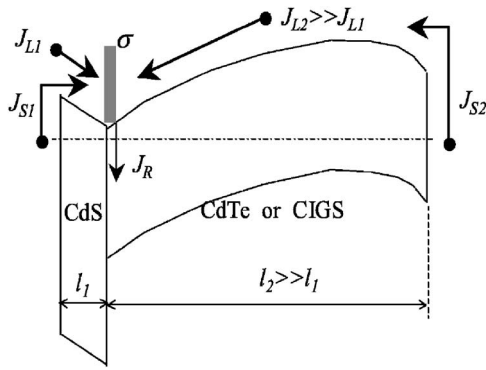


FIG. 2. Phenomenological model of CdS-based thin-film PV.  $\sigma$  represents the two-dimensional electron charge density.  $J_{L1}$ ,  $J_{L2}$  are component 1 and 2 photocurrents,  $J_{s1}$  and  $J_{s2}$  are the corresponding saturation currents.  $J_R$  is the recombination current.

curvature; the depletion widths remain arbitrary within the requirement that they are greater than the corresponding layer thicknesses. Unlike the examples in Fig. 1, our model neglects the back field effects (rightmost part of the diagram).

In this framework, the lack of carrier collection from CdS is due to the field reversal, and the corresponding barrier in Fig. 2 is consistent with the CdS depletion.<sup>10</sup> Under illumination or forward bias, the electrons accumulated in the ‘gull wing’ region will generate the electric-field flattening the singularity and suppressing the barrier. Hence, the electric current increase leading to the dark and light  $J$ - $V$  crossing, qualitatively similar to the CdS photoconductivity. On the other hand, the CdS barrier will limit forward current causing  $J(V)$  flattening (rollover) in the forward bias region.

The model of Fig. 2 allows for a closed-form analytical solution. In addition to the parameters presented in Fig. 2, we introduce the layer dielectric permittivities ( $\epsilon_1$  and  $\epsilon_2$ ), the electron potential barriers ( $V_{B1}$  and  $V_{B2}$ ) measured from the conduction-band singularity, and the barriers ( $W_1$  and  $W_2$ ) determining the saturation currents,  $J_{s1(2)} = J_{s1(2)}^0 \exp(-W_{1(2)}/kT)$ . Here the subscript 1(2) refers to the device component 1(2). Each of the two components is described by its standard diode characteristic  $J_{1(2)} = J_{s1(2)} [\exp(qV_{1(2)}/kT) - 1] - J_{L1(2)}$  with the open-circuit voltage<sup>11</sup>

$$V_{oc1(2)} = \frac{kT}{q} \ln(1 + J_{L1(2)}/J_{s1(2)}). \quad (1)$$

The CdS barrier is relatively low,  $W_1 \ll W_2$  and  $J_{s1} \gg J_{s2}$ . The photocurrent ratio can be estimated as  $J_{L1}/J_{L2} \sim 0.15$  for a thick (up to 0.2 micron) CdS and is smaller for thin CdS.

The electric current continuity requires that  $J = J_1(V_1) = J_2(V_2) + J_R$ , where  $J_R$  is the recombination current,  $V_1$  and  $V_2$  are the electric potential differences across the layers,  $V_1 + V_2 = V$ . The electric potential distribution is found from the electrostatic problem, which simplifies because the electron density is exponentially high in the proximity of ‘gull wing’ singularity and can be approximated by a self-consistent two-dimensional charge density  $\sigma$ ; hence, the electric potential linear in coordinate. In this approximation,  $J_R = \gamma\sigma$ , where  $\gamma$  accounts for the interfacial defect properties. The equilibrium value  $\sigma = \sigma_0$  remains the model parameter.

The problem is further simplified by noting that the recombination is relatively inefficient in device quality structures (say,  $J_R \leq 0.1J_{L2}$ ) and can be treated as perturbation. Namely,  $\sigma$  will be found neglecting the recombination and then substituted into  $J_R = \gamma\sigma$ .

The partial currents can be written in the form:

$$J_{1(2)} = \pm J_{s1(2)} \left[ 1 - \frac{\sigma}{\sigma_0} \exp\left(-\frac{\Delta V_{B1(2)}}{kT}\right) \right] \pm J_{L1(2)}, \quad (2)$$

with (+) corresponding to component 1. The barrier change is expressed through the standard electrostatics

$$\Delta V_{B1(2)} = \pm \frac{Vl}{l_{2(1)}} - \frac{4\pi\sigma ql}{\epsilon}, \quad \epsilon = \frac{\epsilon_1\epsilon_2}{\epsilon_1 + \epsilon_2}, \quad l = \frac{l_1l_2}{l_1 + l_2}. \quad (3)$$

Substituting this into  $J_1 = J_2$  determines the electron charge density  $\sigma$ ,

$$\frac{\sigma}{\sigma_0} \exp\left(\frac{4\pi q\sigma l}{kT\epsilon}\right) = \frac{J_{s1} + J_{s2} + J_{L1} + J_{L2}}{J_{s2} \exp(qVl/kTl_1) + J_{s1} \exp(-qVl/kTl_2)}. \quad (4)$$

Substituting Eqs. (3) and (4) into Eq. (2) yields the integral  $J$ - $V$  characteristics,

$$J = J_{s1} + J_{L1} - \frac{J_{s1} + J_{s2} + J_{L1} + J_{L2}}{1 + (J_{s2}/J_{s1})\exp(qV/kT)} - J_R, \quad (5)$$

with  $J_R = \gamma\sigma$  and  $\sigma$  from Eq. (4). The characteristic in Eq. (5) is mathematically quite different from that of the standard diode leading to a number of predictions, which we list in the approximation  $J_R = 0$  next.

The system open-circuit voltage and short-circuit current are

$$V_{oc} = V_{oc2} - V_{oc1} \quad \text{and} \quad J_{sc} = \frac{J_{L2}J_{s1} - J_{L1}J_{s2}}{J_{s1} + J_{s2}}. \quad (6)$$

Because  $J_{s2}/J_{s1} \ll 1$ , the lack of carrier collection from CdS is predicted ( $J_{sc} \approx J_{L2}$ ). On the other hand, for a blue light illumination fully absorbed in CdS ( $J_{L2} = 0$ ), we predict  $J_{sc} = -J_{L1}$ , hence QE < 0.

The dark to light  $J$ - $V$  crossing takes place at

$$V_X = V_{oc} + \frac{kT}{q} \left[ \exp\left(-\frac{qV_{oc1}}{kT}\right) + \exp\left(-\frac{qV_{oc2}}{kT}\right) \right], \quad (7)$$

slightly above  $V_{oc}$ , consistent with the observations. In addition, Eq. (5) predicts a  $J$ -V rollover more profound at low temperatures, which is indeed observed many times and attributed mostly to the back contact effects.<sup>12</sup>

The slopes  $dV/dJ$  at  $V=0$  and  $V=V_{oc}$  give the short-circuit (“shunt”) and open-circuit (“series”) resistances

$$R_{sc} = \frac{kT(\sqrt{J_{s2}/J_{s1}} + \sqrt{J_{s1}/J_{s2}})^2}{q(J_{s1} + J_{s2} + J_{L1} + J_{L2})}, \quad (8)$$

$$R_{oc} = \frac{kT(J_{s1} + J_{s2} + J_{L1} + J_{L2})}{q(J_{s1} + J_{L1})(J_{s2} + J_{L2})}. \quad (9)$$

Assuming, for example, the typical<sup>2</sup>  $J_{L1} \sim 0.1J_{L2} \sim 2 \text{ mA/cm}^2$  and  $J_{s2} \ll J_{s1} \leq J_{L1}$  yields  $R_{oc} \approx (kT)/(qJ_{L1}) \sim 10 \Omega$ , in the ballpark of the observed series resistances for CIGS (Ref. 13) and CdTe (Ref. 14) based PV. This estimate

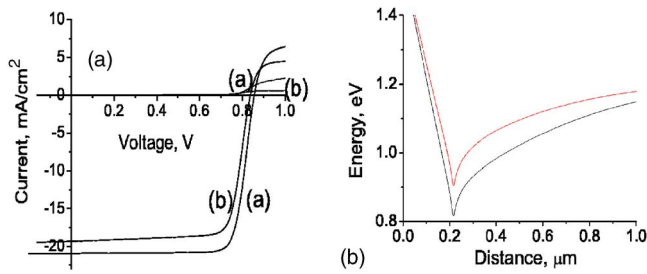


FIG. 3. Left: AMPS simulated (a) vs analytical (b)  $J$ - $V$  characteristics for the same band diagram. Right: The proximity of conduction-band singularity simulated by AMPS for the forward bias of 1 V in the dark and 1.5 AM light. (The “cusp” artifact is due to the artificial doped layer.) In this modeling, the back barrier effects and recombination were eliminated; hence,  $J$ - $V$  crossing and rollover are due to the CdS barrier. Nevertheless, the device parameters  $V_{oc}=0.81$  eV,  $J_{sc}=20$  mA/cm<sup>2</sup>, fill factor of 72%, and efficiency 12.8% appear realistic for CdTe PVs.

changes when the alternative inequality  $J_{L1} \ll J_{s1}$  takes place. In addition, the measured resistances can be affected by factors beyond the present model, such as the back field<sup>12</sup> and nonuniformity.<sup>15</sup> Defect-assisted tunneling (hopping) transport through the CdS barrier would also have a noticeable effect on the above predictions. Nevertheless, Eqs. (5)–(8) call upon experimental verifications including the temperature, light intensity, and spectra dependencies.

Consider briefly the recombination effects. Equation (4) predicts that  $\sigma$ , and thus  $J_R$  is a maximum at

$$V_R = \frac{kT}{q} \ln \left( \frac{J_{s1} l_1}{J_{s2} l_2} \right) \approx V_{oc} - \frac{kT}{q} \ln \left( \frac{J_{L2} l_2}{J_{L1} l_1} \right). \quad (10)$$

Assuming the typical  $J_{L1} l_1 / J_{L2} l_2 \leq 0.01$ , one can estimate  $V_R \approx V_{oc} - 0.06$  eV. For realistic  $l_1 / l_2 \leq 0.1$ , it follows from Eq. (4) that  $J(R)$  drops sharply when  $V > V_R$ , while it decreases rather slowly for  $V < V_R$ . In other words, the recombination has almost no effect on the  $J$ - $V$  curve when  $V > V_R$ , while it decreases  $|J|$  almost uniformly when  $V < V_R$ .

We verified our findings with numerical AMPS simulations. Two artificial narrow layers (10% of CdS thickness) containing high concentrations ( $10^{18}$  cm<sup>-3</sup>) of shallow donors and acceptors were added on the opposite sides of the original CdS to model the built-in reversal electric field in CdS. In the spirit of this model, we did not include the buffer layer, back field, and any recombination centers. As is seen from Fig. 3, the analytical and numerically simulated curves are reasonably close. The observed deviations appear legitimate, since our analytical result does not account for the carrier diffusion.

Overall, our model emphasizes interfacial properties, such as the interfacial morphology, related compression, and charges. In the terms of practical implications, they can be altered by tuning the deposition regimes, creating doping-induced stresses, and applying proper interfacial treatments (layers).

In conclusion, we have proposed a physical model that explains a variety of facts for CdS-based PVs. This model is solved analytically. The predicted properties differ considerably from that of the standard  $p$ - $n$  junction and call upon further experimental verifications.

The authors are grateful to A. L. Fahrenbruch who suggested the method of AMPS modeling of interfacial charge effects. Also, they acknowledge useful discussions with D. Shvydka, J. Drayton, and A. D. Compaan. This work was partially supported by the NREL (Grant No. RXL-5-44205-01).

<sup>1</sup>B. von Roedern, K. Zweibel, and H. S. Ullal, in *Proceedings 31th IEEE Photovoltaic Specialists Conference*, Coronado Springs, FL, 3–7 January 2005 (IEEE, Piscataway, NJ, 2005), p. 183.

<sup>2</sup>W. N. Shafarman and L. Stolt, in *Handbook of Photovoltaic Science and Engineering*, edited by A. Lique and S. Hegedus (Wiley, Chichester, 2003), p. 183; B. E. McCandless and J. R. Sites, *ibid.* p. 617.

<sup>3</sup>M. Gloeckler, A. L. Fahrenbruch, and J. R. Sites, in *Proceedings of the 3rd World Conference on Photovoltaic Energy Conversion*, Osaka, Japan, 11–18 May 2003 (IEEE, Piscataway, NJ, 2003), p. 491.

<sup>4</sup>AMPS is a software package developed by Penn State University and aimed at simulating semiconductor multilayer devices; available at <http://www.psu.edu/dept/AMPS>.

<sup>5</sup>D. Shvydka, J. Drayton, A. D. Compaan, and V. G. Karpov, *Appl. Phys. Lett.* **87**, 123505 (2005).

<sup>6</sup>Y. Roussillon, D. Giolando, D. Shvydka, A. D. Compaan, and V. G. Karpov, *Appl. Phys. Lett.* **84**, 616 (2004).

<sup>7</sup>K. Barri, S. Bapanapalli, S. Gayam, M. Jayabal, L. Nemani, Y. Venkatraman, H. Zhao, D. L. Morel, and C. S. Ferekides, private communication; see: [www.nrel.gov/ncpv/thin\\_film/docs/DevPhys-Ferekides.ppt](http://www.nrel.gov/ncpv/thin_film/docs/DevPhys-Ferekides.ppt).

<sup>8</sup>S. Hegedus and B. McCandless (private communication); *National CdTe R&D Team Meeting Minutes*, edited by P. V. Meyers and H. S. Ullal, 27–28 January 2000 (NREL, Golden, CO, 2000), Appendix 12.

<sup>9</sup>S. Hegedus, D. Ryan, K. Dobson, B. McCandless, and D. Desai, *Mater. Res. Soc. Symp. Proc.* **763**, B9.5.1 (2005).

<sup>10</sup>Based on different argument, the concept of CdS related barrier was suggested in G. Agostinelli, D. L. Bätzner, and M. Burgelman, *Thin Solid Films* **431**, 407 (2003).

<sup>11</sup>S. M. Sze, *Physics of Semiconductor Devices* (Wiley, New York, 1981).

<sup>12</sup>Y. Roussillon, V. G. Karpov, D. Shvydka, J. Drayton, and A. D. Compaan, *J. Appl. Phys.* **96**, 7283 (2004).

<sup>13</sup>D. Liao and A. Rockett, in *Proceedings of the 28th IEEE Photovoltaic Specialists Conference*, Anchorage, AL, 15–22 September 2000 (IEEE, Piscataway, NJ, 2000), p. 446.

<sup>14</sup>X. Li, D. W. Niles, F. S. Hasoon, R. J. Matson, and P. Sheldon, *J. Vac. Sci. Technol. A* **17**, 805 (1999).

<sup>15</sup>V. G. Karpov, A. D. Compaan, and D. Shvydka, *Phys. Rev. B* **69**, 045325 (2004).